Atomic relaxation and dynamical generation of ordered and disordered chemical vapour infiltration (CVI) SiC polytypes

Gerard L. Vignoles

Atomic relaxation and dynamical generation of ordered and disordered chemical vapour infiltration (CVI) SiC polytypes

G. L. VIGNOLES
Laboratoire des Composites ThermoStructuraux
3,Allée La Boëtie – Université Bordeaux 1
F33600 PESSAC, France
vinhola@lcts.u-bordeaux1.fr

Published in
Journal of Crystal Growth,
vol. **118** (1992), pp. 430-438.

Atomic relaxation and dynamical generation of ordered and disordered chemical vapour infiltration (CVI) SiC polytypes

G. L. VIGNOLES

Abstract.

The coexistence of ordered and disordered polytypes in SiC deposits is discussed from the point of view of their formation under CVD/CVI conditions, i.e., far from equilibrium. Local deformations at layer *n* are considered to determine the orientation and the deformations of the $(n + 1)^{th}$ layer. An analysis of this dependence is made by constructing a first return map of an atomic relaxation variable, based on the *ab initio* calculation data for some regular polytypes made by Cheng et al.,[*J. Phys. (Condens. Matter)* **2** (1990) 5115]. Orientation sequences are linked to the local deformation parameter, and to ^{29}Si and ^{13}C NMR shifts. Iterations of this map are considered as a one-dimensional dynamical system simulating layer-by-layer growth. Depending on control parameters, the dynamical system exhibits stationary, periodic or chaotic orientation sequences, reproducing many experimentally obtained polytypes. The occurrence of CVD- or CVI-grown one-dimensionally disordered polytypes can thus possibly arise from a deterministic process able to yield also regular structures for nearby values of control parameters.

TEXT.

1. INTRODUCTION

In view of the potential high-temperature applications of silicon carbide (*e.g.* in ceramic- ceramic composites or electronic devices), its crystal structure has been thoroughly investigated, revealing that *SiC* can be grown in a very wide variety of polytypic modifications (more than 250) [1-3]. In addition to short- and long-period polytypes of *SiC*, there also exist the so-called “one-dimensionally disordered” ones [3-5], some of the latter having been obtained by means of the chemical vapour deposition (CVD) or infiltration (CVI) process [6,7]. Although many attempts have been made to explain the occurrence of polytypism (one-dimensional polymorphism), no model accounting simultaneously for the occurrence of both ordered and disordered polytypes has been proposed [8-10]. The aim of the present contribution is to suggest a new way of studying the origin of disordered as well as

periodic polytypes specific to synthesis processes far from equilibrium. This work is based on a dynamical approach, which has already shown great promise in the setting up of deterministic models of complicated or chaotic behaviour [11], as seems to be the case in CVD- or CVI-grown *SiC*. No attempt will be made to discuss the thermodynamic global stability of the structures: this problem has already been dealt with [10]. On the other hand, it will be shown how disordered polytypes can appear from deterministic growth mechanisms yielding also the most commonly reported periodic polytypes. These structures, obtained at rather high temperatures, are assumed to be observable if cooled rapidly enough.

2. POLYTYPE DESCRIPTION

Silicon carbide polytypes may be described as different stacking sequences of SiC layers along a $(111)_\alpha$ or the $(0001)_\beta$ direction of the corresponding cubic or hexagonal structures which are also the only growth directions of interest to control polytypism [1,2,12]. Each layer actually consists of two sublayers, one of pure *Si* and the other of pure *C*, both in a hexagonal arrangement [13]. A schematic representation is shown in fig. 1. During the growth process, every new layer has a choice in its stacking position: it is either a continuation of the former orientation, plus a translation, or is in the symmetrical orientation, with both translation and 180° rotation. This "choice" point of view is consistent with the "***h*-*k***" notation used by Jagodzinski to describe polytype sequences [14], ***h*** being associated with both translation and rotation and ***k*** with pure translation. As it is apparent from fig. 1, these two orientations lead to non-equivalent atomic neighbourhoods: if the new layer has ***h*** orientation the atoms of its upper sublayer are in eclipsed conformation with respect to the atoms of the lower sublayer of the preceding layers, *i.e.*, their third neighbours along the growth axis, while in ***k*** orientation, they are staggered [15]. Each polytype, ordered or not, can be described by an orientation sequence U_n , n

being the integer layer index (here equivalent to a discrete time parameter), *e.g.*, the 15R polytype, whose Zhdanov notation [16] is $(23)_3$, will be denoted $(\boldsymbol{hkhkk})_3$. U_n is a Boolean sequence.

3. LOCAL DEFORMATIONS

All polytypes, except the purely cubic structures, exhibit deviations from their associated ideal structure. The projections on the growth axis of the atomic spacings are not necessarily equal from one layer to another: indeed the coordination tetrahedra of every atom can be distorted along this direction, usually retaining its threefold symmetry axis parallel to it [15]. This feature has been evidenced in the case of *SiC* by different methods. Careful X-ray investigations of 2H-*SiC* [17] and 6H-*SiC* [18] have led to estimates of non-ideal bond lengths and angles in the bulk structure. ^{29}Si and ^{13}C NMR studies [19] reported the existence of different kinds of sites in common polytypes (3C, 4H, 6H, 15R), and have been related to the orientations of their layer and the neighbouring ones [19,20]. *Ab initio* pseudopotential calculations including relaxation effects have been made for 3C, 2H, 4H, 6H and 15R structures [21]: they led to an estimation of the bond lengths in reasonable agreement with the X-ray data, mainly for the 6H polytype. The bond lengths have been reported to vary always by less than 3% from ideal ones, and the angles by lesser amounts [15,21].

The characteristic geometrical variables of each layer (regardless of specific surface modifications due to dangling bonds rearrangements) are three: the length L_n of the *Si-C* bond parallel to the growth axis; the length l_n of the three remaining *Si-C* bonds and the angle A_n between L_n and l_n as shown in fig. 2. However if all the layers are in epitaxial relationship with the preceding ones, the $\boldsymbol{a}$ parameter of the equivalent hexagonal unit cell is constant and equal to 3/2 times $l_n \sin(A_n)$. This implies that only one of the two variables l_n and A_n has to be considered.

4. THE ITERATIVE MODEL

Different orientations are related to different atomic environments and consequently to different interatomic interactions such as electrostatic or Van der Waals ones. At first sight it could be thought that such interactions should always favour the same orientation but this is not experimentally the case. In order to link the orientation variability to energetic factors one has to admit that the latter are not constant. Actually, this degree of freedom is provided by the possibility of tetrahedron deformations.

As seen before, the ***h*** and ***k*** sites begin to be distinguishable if one considers their third or further neighbours. Indeed, Cheng *et al*. [21] have tried to reach the force field induced in a purely cubic crystal by a single ***h*** layer, and have found that this field presented a maximum at the positions which were next-nearest to the centre of the stacking fault, *i.e.*, at atoms which are third neighbours to each other. As the force field is rapidly decreasing beyond these positions it is a good approximation to restrict the model to the range of this effect.

At CVI temperatures (~ 1300 *K*), *i.e.* far be- low the melting point of *SiC* (~ 2800 *K*), most of the growing crystal is not able to rearrange itself: this is why the growth occurs far from global equilibrium. Once a layer has chosen its orientation it becomes "frozen" after another or several other layers have stacked upon it. On the other hand, if the temperature is high enough, the upper atoms of the new layer may "oscillate" some time before choosing the most energetically favoured position: *i.e.*, local equilibrium is attained for the mere newest layer. Working on the assumption of last-layer local equilibrium and discarding consideration of the global equilibrium is thus consistent with the usual CVD or CVI conditions. The mathematical framework of a simple, local layer-by-layer growth model accounting for orientation instability can be built out of these hypotheses.

The surface is considered to be represented by the atoms of the last layer of index n. For simplicity it is supposed that they exhibit the same behaviour as in the bulk structure. As the a parameter is fixed the layer is characterized by two independent variables, *e.g.* l_n and L_n . Let then come from an infinite distance the (bare) Si and C atoms that are going to form the next bilayer. At this point the orientation choice appears: the atoms of the upper layer may lie exactly over their third neighbours (***h***, or eclipsed), or exactly over the barycentre of triplets of them (***k***, or staggered). The proper energetic calculations (i.e. accounting for third-neighbour interactions at least) made in both cases allowing only the impinging atoms to relax lead to two different energy values, $E_{n+1,\boldsymbol{h}}$ and $E_{n+1,\boldsymbol{k}}$. The lowest of them is actually retained as the effective E_{n+1}. The corresponding orientation is then U_{n+1} and the corresponding lengths are l_{n+1} and L_{n+1}, from which the whole procedure may be iterated to determine U_{n+2}, l_{n+2} and L_{n+2} and so on.

The growth is thus described by the repetition of a calculation using l_n and L_n to evaluate U_{n+1} , l_{n+1} and L_{n+1}: it can be thought of as a mapping of some part of $\mathbb{R}^2$ (*i.e.*, the (l_n , L_n) space) into itself from which the boolean sequence can be extracted. It should be stressed that this simplified description, as it neglects interaction beyond third neighbours, does not relate directly the orientation of the new layer to the orientation of the previous one, but to its deformations. However it will be seen in the next section that ***h*** and ***k*** orientations of the n^{th} layer correspond to two well-separated groups of deformation values for the same layer.

The energy value E_n represents an evaluation of the total energy of the n^{th} layer: it has been presented in previous works dealing with thermodynamic stability of periodic structures [10], as a discrete quantity, while the present model does not. Actually there is no contradiction: if the above model displays periodic behaviour the E_n values will indeed belong to a finite set. Moreover, they are always very close to the

mean value, varying from it by quantities at most 10^{-5} times lower. One can doubt the efficiency of such fine effects; but the point is that the absolute value of the total layer energies is not directly involved in the orientation choice: on the contrary, this choice is ruled by a difference between two such energies.

5. DEFORMATION SEQUENCES: A PHENOMENOLOGICAL APPROACH TO AN ITERATED MAP

With the aim of acquiring better knowledge of the iterative process, it has been tried to reach it using the results of relaxed structures calculations by Cheng et al. [21], in a one-dimensional simplification for the sake of a simpler discussion without loosing any general qualitative result.

The *ab initio* values of l_n and L_n as calculated in ref. [21] for polytypes 3C, 2H, 4H, 6H and 15R, are reported at table 1 together with the corresponding orientations (that is, U_n values). All the (l_n , L_n) couples are plotted in fig. 3, as a phase space representation of a 2D mapping. It is clearly seen that the points are dispersed along a particular direction, so that the mapping looks quite one-dimensional. It is thus proposed to study the behaviour of the only variable $\delta_n = l_n / L_n - 1$ which retains the essential features of the deformations. As a convention δ_n is a measure of the deformation of the coordination tetrahedron of the *C* atoms when considering growth by the silicon face (the orientation choice is a position choice for the *Si* atoms).

It is easy to see that all δ_n are positive: this feature corresponds to an elongation along the growth axis. Moreover the δ_n values are more important for all the ***h*** layers ($\delta_n >$ 0,4%) than for the ***k*** layers ($\delta_n < 0.2\%$). The ***h*** orientation corresponds to stronger deformations than the ***k*** orientation, a general fact about zincblende/ würtzite polytypism [15]. At short distances, steric repulsions between third neighbours in ***h*** disfavour this conformation, but if the distance grows (longitudinal elongation),

electrostatic attraction (the ionicity of *SiC* has been shown to be rather important [22)) has the opposite effect. Because of the balancing effects of these two interactions, the choice of orientation is very sensitive to interatomic distances.
In order to determine whether there is an underlying logic in the δ_n sequences or not a plot has been made of δ_{n+1} versus δ_n as a first return map of the process, in fig. 4. Remembering that all the points do not correspond to the same value of parameter ***a***, one can think of fitting to them some curve, which would be the graphical plot of an underlying function *f*: $\delta_n \rightarrow \delta_{n+1}$ Unfortunately it does not appear as being too smooth a curve, however, the presence of a discontinuity is partly justified by the study of the relation between deformations and orientation sequences.

6. SYMBOLIC DYNAMICS AND ORIENTATION SEQUENCES

It has already been mentioned that the δ_n values are very neatly split into two groups, one of ***h*** orientation and one of ***k*** orientation. More precisely the first return map suggests to divide them into four groups, on the criterion of both U_n and U_{n+1} . These groups may be referred to as A, B, C and D in exact agreement with the groups of chemical shifts in silicon carbide NMR [19,20]. Going further these groups are split again on the criterion of U_{n+2}, as shown in fig. 5. This is consistent with the observed differences between the group A chemical shifts of 3C (***k****kk*) and of 6H or 15R (***k****kh*) and a suggestion that a more refined NMR study of *SiC* would lead to recognize further splittings of the chemical shift groups [20]. The ordering of the $U_n U_{n+1} U_{n+2}$ sequences following δ_n is particularly regular: if one replaces ***k*** with 0 and ***h*** with 1 then it is exactly the ordering of binary numbers: 000 < 001 < 010 < … .
It is of interest to look at what happens if this ordering holds for sequences of arbitrary lengths in the spirit of the encoding procedure for unimodal maps [23,24]. Let any sequence U = $U_1 U_2$ … represent a real number of the interval [0;1],

replacing ***k*** with 0 and ***h*** with 1 (*e.g.* ***khk*** represents 0.010 in binary representation or 0.25 in decimal representation). The real number x associated to U is written $r(U)$, and U is equal to $S(x)$. Then the above correspondence between sequence ordering and real numbers ordering is kept. Let $\sigma(U) = U_2 U_3 \ldots$ be the shifted U sequence, it is easy to see that the shift operation of the sequences corresponds to a function of [0,1] into and onto itself namely:

$$r(\sigma(U)) = T(r(U)) \qquad \text{or} \qquad r(\sigma(S(x))) = T(x) \qquad (1)$$

where

$$T(x) = \begin{cases} 2x & \text{if } x \in [0;1/2], \\ 2x-1 & \text{if } x \in [1/2;1], \end{cases} \qquad (2)$$

$T(x)$ is nothing else than a “sawtooth” map, *i.e.*, a once discontinuous map, strictly increasing on the intervals where it is continuous; its shape is very similar to the guessed shape of f in fig. 4.

It is to notice that the binary representation of any real number strictly inferior to 1/2 begins with 0, and with 1 if it is superior to 1/2, exactly as the δ_n values inferior to 0.2% are associated to ***k*** and δ_n values superior to 0.4% to ***h***. Similarly to the case of unimodal maps [24] and of the so-called “gap maps" [25-27], we can derive symbolic dynamics out of the “sawtooth-like”' function by defining a critical value 1/2 and associating the value U_n = ***k*** (or 0) when $x < 1/2$ and U_n = ***h*** (or 1) when $x > 1/2$. Then any point x of [0;1] is such that its binary representation is equal to the sequence of 0s and ls obtained by iterating this point under T. From this fact one expects T (and f) to belong to a family of maps which should exhibit the same potentiality of dynamical behaviour as families of gap maps.

7. AN EXAMPLE OF GENERATION OF POLYTYPES WITH THE SAWTOOTH MAP FAMILY

Once a general shape for the mapping for the dynamical system has been determined it is of interest to study the variation of its behaviour according to external conditions. As an example, tests are performed on a one-parameter family of mappings whose analytical expression is simple and whose global shape is of the desired form.
The following family has been used:

$$f_\lambda(x) = \begin{cases} 4\lambda x(1-x) & \text{if } x \in [0;1/2] \\ 1-4\sqrt{\lambda}\,x(1-x) & \text{if } x \in [1/2;1] \end{cases} \qquad (3)$$

Provided $0 \leq \lambda \leq 1$, the f_λ are endomorphisms of [0,1] into itself. These functions fulfil the condition of negative Schwartzian derivative [28]: although there is no rigorous demonstration that it is a sufficient condition for them to display at most one limit cycle, it has been observed numerically to be the case. The parameter dependence of f_λ is not symmetrical from one side of l /2 to the other, a fact that is more representative of the general case. The shape of these functions consists of two portions of a parabola, as shown in fig. 6.
The bifurcation diagram of this family is sketched in fig. 7: it is somewhat more complex than the well-known bifurcation diagram of the logistic map [11,23]; as a matter of fact, it does not display any period-doubling cascade. The 3C and 2H polytypes correspond to the trivial cases where there are fixed points in the ***k*** or ***h*** regions. Many odd-period cycles appear in this diagram. In particular the cycles whose sequences correspond to polytypes 6H and 15R have a very broad stability domain, Some long-period cycles appear too, consisting mainly of sequences of ***hk***s and ***hkk***s (i.e., of 2s and 3s in Zhdanov notation [16]), as it is the case for most known polytypes of *SiC*. Some of these cycles yield experimentally observed polytypes, some others do not. For higher values of λ aperiodic sequences appear, still with periodic windows inside the domain. As λ grows, the chaotic sequences contain less sequences of 2s and 3s and more sequences of 1s, 4s and more, tending to a more

random-like behaviour.

The above model, though very approximate, is thus able to reproduce qualitatively the richness of *SiC* polytypism: fixed points (3C or 2H), periodic cycles (abundant polytypes as 6H and 15R, and longer-period ones consisting of sequences of 2s and 3s), and aperiodic structures.

The mathematical characterization of periodicity, aperiodicity and their frequencies is based on the so-called kneading theory [29,30,23]. Methods used to study the existence of chaos for the two-parameter family of gap maps [25-27] are easy to adapt to the sawtooth map case, confirming the fundamental fact of the set-up of chaotic structures in a deterministic growth model (sec appendix).

8. CONCLUSION

This work has dealt with the polytypism of *SiC* considered as a result of an out-of-equilibrium growth process in CVD or CVI conditions. A study of interlaced interactions and their relation with the deformations of the atomic coordination tetrahedra has led to the building of a local recurrent law yielding deformation and orientation sequences. A closely related one-parameter family of real line mappings shows indeed most qualitative features of the richness of *SiC* polytypism. The occurrence of one-dimensional disordered polytypes is shown to be described by a deterministic model accounting also for the existence of regular structures, and related only to interatomic interactions during the growth. In one sense, the disorder is explained as an event inherent to the growth process.

The goal in this work was to establish a general frame for a dynamical description of polytypism; further studies have to be carried out in several directional to achieve a more precise understanding of the phenomenon. As the central physical basis of the model are the sequences of tetrahedron deformations: more information about them is still needed either experimentally, or out of proper simulations. The links with

external parameters have to be enlightened through more precise descriptions including “horizontal” effects (*e.g.*, surface rearrangements during the growth, step inclusion, spiral growth, etc.),“chemical” effects (impingement of molecules, instead of bare atoms, with subsequent surface reactions leading to inclusion) and accounting for activation barriers.

ACKNOWLEDGEMENTS

This work has been supported by SEP and CNRS through a grant given to the author. The author is indebted to Mrs. S. Schamm (CEMES-LOE, Toulouse) for helpful discussions.

APPENDIX: THE KNEADING THEORY FOR THE SAWTOOTH MAP

In the following part, an itinerary will be considercd as a sequence of $\boldsymbol{h}$ ($x > x^*$), $\boldsymbol{k}$ ($x < x^*$) or $\boldsymbol{o}$ ($x = x^*$), and the kneading sequences K_+ and K_- are associated to the itineraries of $f(x^*_+)$ and $f(x^*_-)$. The ordering of sequences is an extension of the rule given in the main part:

$$\boldsymbol{k} < \boldsymbol{o} < \boldsymbol{h} \qquad \text{(A.1)}$$

$$\mathrm{I}\boldsymbol{k} < \boldsymbol{o} < \mathrm{I}\boldsymbol{h} \quad \text{for any sequence I.} \qquad \text{(A.2)}$$

No consideration of parity of any sequence is necessary here, in contrast to the case of unimodal [23] and gap [26] maps.

Any sawtooth map, analogously to the gap maps, is characterized by a couple (K_+,K_-) of kneading sequences, which determine admissibility conditions for any itinerary I :

$$\mathsf{L}(I) \leq K_- \quad \text{and} \quad \mathsf{R}(I) \geq K_+ \qquad \text{(A.3)}$$

where $\mathsf{L}(I)$ (respectively $\mathsf{R}(I)$) is the set of all subsequences of I that follow the letter $\boldsymbol{k}$ (respectively $\boldsymbol{h}$). As an immediate consequence, all allowed K_- are $\geq \boldsymbol{o}$, with the exception of $\boldsymbol{k}^\infty$ and all allowed K_+ are $\leq \boldsymbol{o}$, with the exception of $\boldsymbol{h}^\infty$. As in ref. [32], it is possible to build a skeleton in the (K_-, K_+) plane: the obtained structure is symmetrical with respect to an exchange of $\boldsymbol{h}$ with $\boldsymbol{k}$ and K_- with K_+. All the rules of construction are analogous, leading to the same conclusions as for the gap maps, and mainly the existence of a threshold for chaos is proved. The demonstrations concerning the existence of the threshold are contained in ref. [26], so it is unnecessary to display them here.

REFERENCES

[1] A.R. Verma and P. Krishna, "Polymorphism and Polytypism in Crystals" (Wiley, New York, 1966).

[2] P. Krishna, Ed., "Crystal Growth and Characterization of Polytype Structures" (Pergamon, Oxford, 1983).

[3] G.R. Fisher and P. Barnes, *Phil. Mag. B* **61** (1990) 217.

[4] H. Sato and S. Shinozaki , *Mater. Res. Bull.* **10** (1975) 157;
S. Shinozaki and H. Sato, *J . Am . Ceram . Soc.* **61** (1978) 425;
S . Shinozaki and K.R. Kinsman, *Acta Met.* **26** (1978) 769.

[5] S. Schamm, R. Mazel, D. Dorignac and J . Sévely, in "Matériaux Composites pour Applications Hautes Températures", Eds. R. Naslain. J. Lamalle and J.L. Zulian (AMAC/CODEMAC, Bordeaux, 1990) p. 207.

[6] E. Fitzer, D. Hagen and H. Strohmeier, *Rev. Intern. Hautes Temp. Réfractaires* **17** (1980) 23 ;
D.P. Stinton, A.J. Caputo and R.A. Lowden, *Am. Ceram. Soc. Bull.* **65** (1986) 347.

[7] R. Naslain and F. Langlais, in: "Tailoring Multiphase and Composite Ceramics", *Materials Science Research* Vol. **20**, Eds. R.E. Tressler et al. (1986) p. 145.

[8] D. Pandey and R. Krishna, in ref. [2], p. 213.

[9] C. Cheng et al., *Phase Transitions* **16-17** (1989) 263.

[10] C. Cheng, V. Heine and I.L. Jones, *J. Phys.: Cond. Mat.* **2** (1990) 5097.

[11] R .M. May, Nature **261** (1976) 459.
[12] A.R. Verma, “Crystal Growth and Dislocations” (Butterworths, London, 1953).
[13] W.F. Knippenberg, *Philips Res*. *Rept*. **18** (1963)161.
[14] H. Jagodzinski, *Acta Cryst.* **2** (1949) 201; *Acta Cryst.* **7**(1954)300.
[15] W. Weltner, Jr., *J. Chem. Phys.* **51** (1969) 2469.
[16] G.S. Zhdanov, *Compt. Rend. Acad. Sci. URSS* **48** (1945) 43.
[17] H. Schultz and K.H. Thiemann, *Solid State Commun.* **32** (1979) 783.
[18] A.H. Gomes de Mesquita, *Acta Cryst.* **23** (1967) 610.
[19] J.R. Guth and W.T. Petuskey. J. Phys. Chem. **91** (1987) 33 ;
J.S. Hartmann *et al .*, *J. Am. Chem. Soc*. **109** (1987) 6059 ;
D.C. Apperley *et al*., *J. Am. Ceram. Soc*. **74** (1991) 777.
[20] M. O'Keeffe, *Chem. Mater.* **3** (1991) 332.
[21] C. Cheng, V. Heine and R. Needs, *J. Phys.: Cond. Mat*. **2** (1990) 5115.
[22] N. Churcher, K. Kunc and V. Heine, *J . Phys. C (Solid. State Phys.)* **19** (1986) 4413.
[23] P. Collet and J.-P. Eckmann, “Iterated Maps on the Interval as Dynamical Systems”, *Progress in Physics* **1** (Birkhaüser, Basel-Boston-Stuttgart, l 980).
[24] S. Isola and A. Politti, *J. Stat. Phys.* **61** (1994) 263.
[25] M.C. de Sousa Vieira, E.Laso and C. Tsallis, *Phys. Rev.* **A** 35 (1987) 945.
[26] W.-M. Zheng, *Phys. Rev*. *A* **39** (1989) 6608.
[27] W.-M. Zheng and L.S. Lu, *Commun. Theor. Phys.* **15** (1991) 161.
[28] D. Singer, *SIAM J . Appl. Math*. **35** (1978) 260.
[29] J. Guckenheimer, *Commun. Math. Phys.* **70** (1979) 133.
[30] J. Milnor and W. Thurston, in: ”Dynamical Systems”, Lecture Notes in Mathematics Vol . **1342**, Ed . J.C. Alexander (Springer, Berlin, 1988).

TABLE CAPTION

Table 1. Variation from the ideal value l_0 of the bond lengths L_n and l_n in relaxed polytypes, as calculated in ref. [21], with associated orientations and deformations parameters δ_n.

TABLE

Polytype	U_n	L_n-l_0 (%)	l_n-l_0 (%)	δ_n(%)
3C	***k***	0	0	0
2H	***h***	0.595	-0.144	0.740
4H	***h***	0.460	-0.121	0.582
	k	0.138	-0.051	0.189
6H	***h***	0.404	-0.086	0.490
	k	0.104	-0.023	0.127
	k	0.102	-0.066	0.168
15R	***h***	0.460	-0.136	0.597
	k	0.140	-0.022	0.162
	h	0.400	-0.161	0.562
	k	0.100	-0.011	0.111
	k	0.100	-0.096	0.196

FIGURE CAPTIONS

Figure 1. Schematic description of a disordered *SiC* polytype observed along a $\langle 11\bar{2}0 \rangle_\alpha$ direction

Figure 2. One bilayer and its associated geometric values

Figure 3. Representation of the layers of simple polytypes as points in the (L_n,l_n) phase space.

Figure 4. First return map of the deformations δ_n (in %). The letters A,B,C,D refer to the NMR shift groups of ref. [19].

Figure 5. Correspondence between the deformations δ_n , the orientation sequences $U_nU_{n+1}U_{n+2}\ldots$ and the NMR shift groups of ref. [19].

Figure 6. Sketches of f_λ for different λ, with associated permanent regimes. (a) λ = 0.6, period 3 cycle with sequence ***hkk***, corresponding to the 6H polytype. (b) λ = 0.7, period 5 cycle with sequence ***hkkhk***, corresponding to the 15R polytype. (c) λ = 0.83, period 2 cycle with sequence ***hk***, corresponding to the 4H polytype. (d) λ = 0.9, aperiodic behaviour, corresponding to one-dimensional disorder.

Figure 7. Bifurcation diagram of f_λ. The dashed line separates points in ***h*** and ***k*** regions.

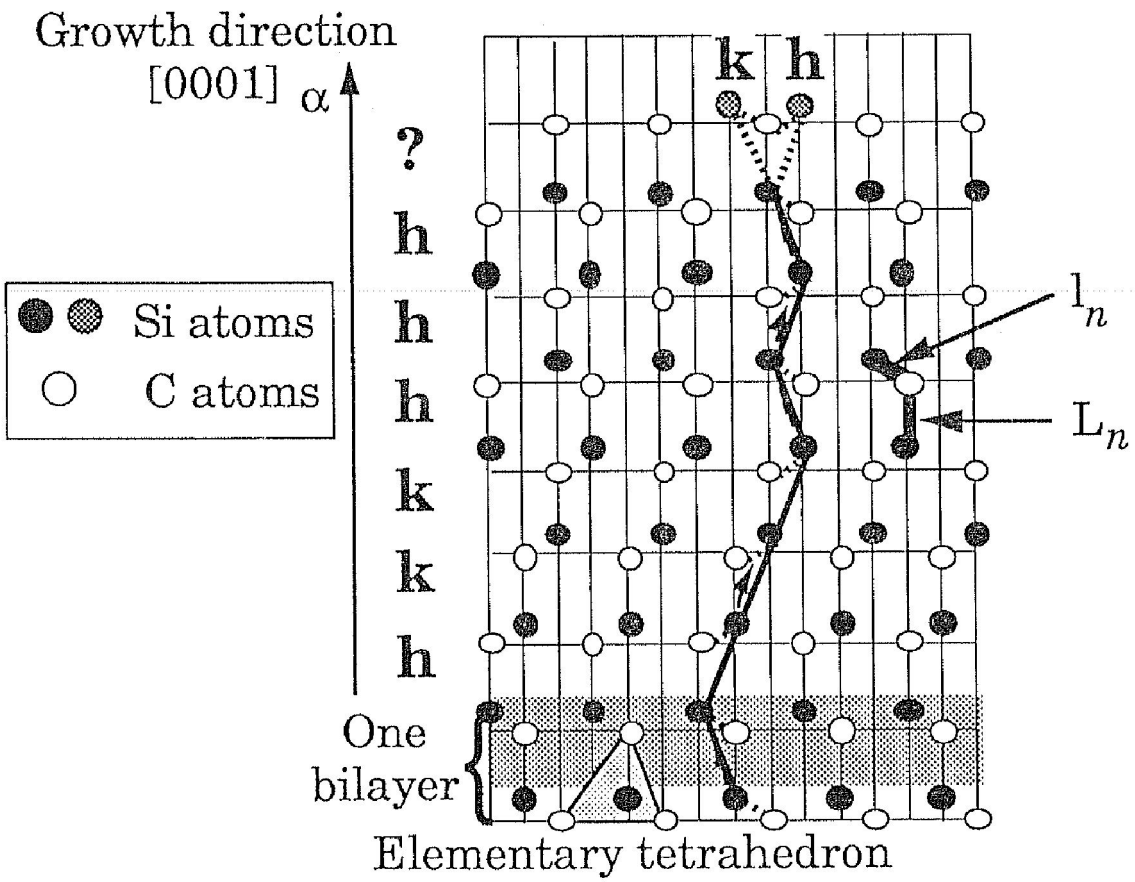
Growth direction
[0001] α
Si atoms
C atoms
?
h
h
h
k
k
h
k h
l_n
L_n
One
bilayer
Elementary tetrahedron

Figure 1.

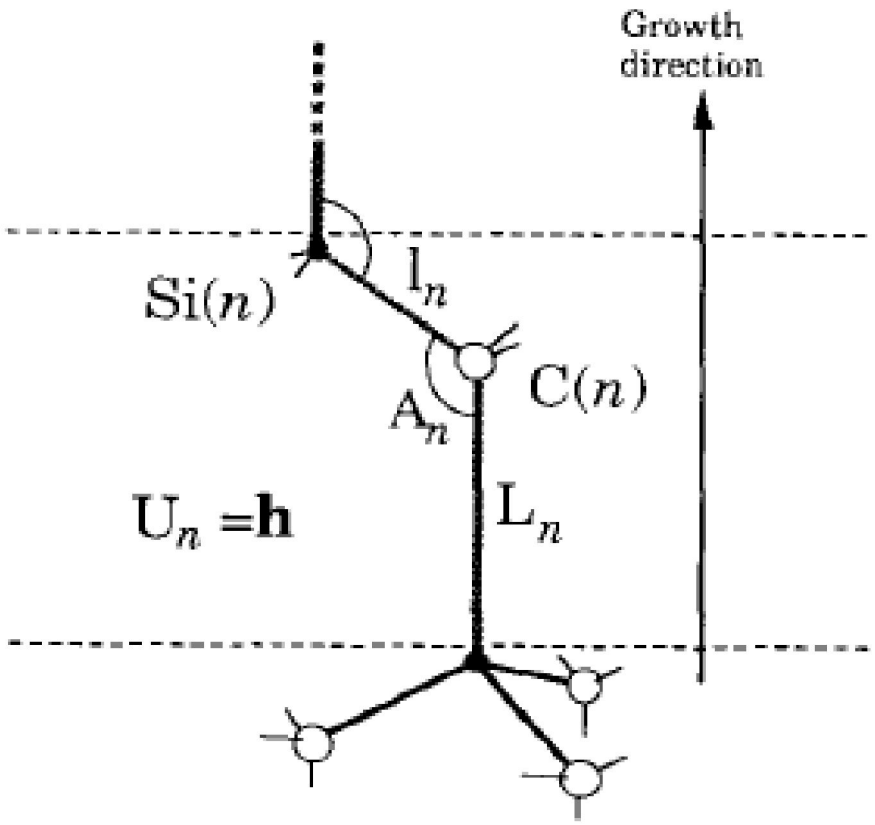

Figure 2.

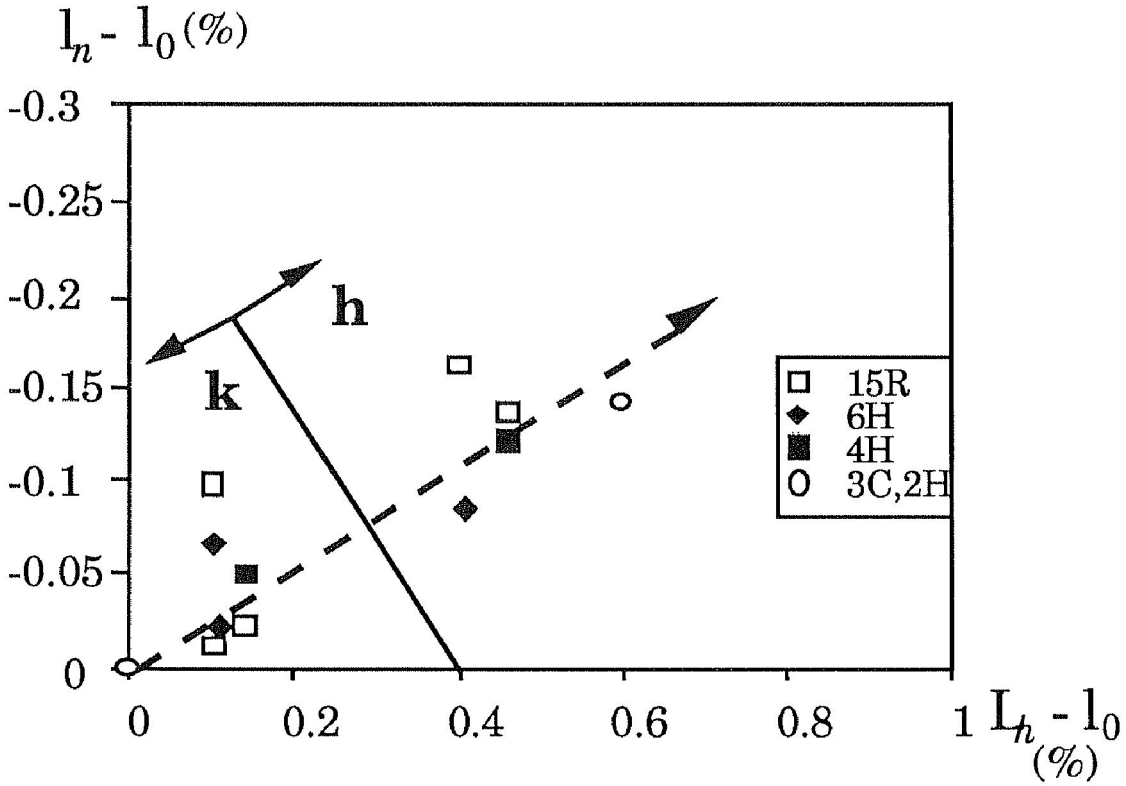

Figure 3.

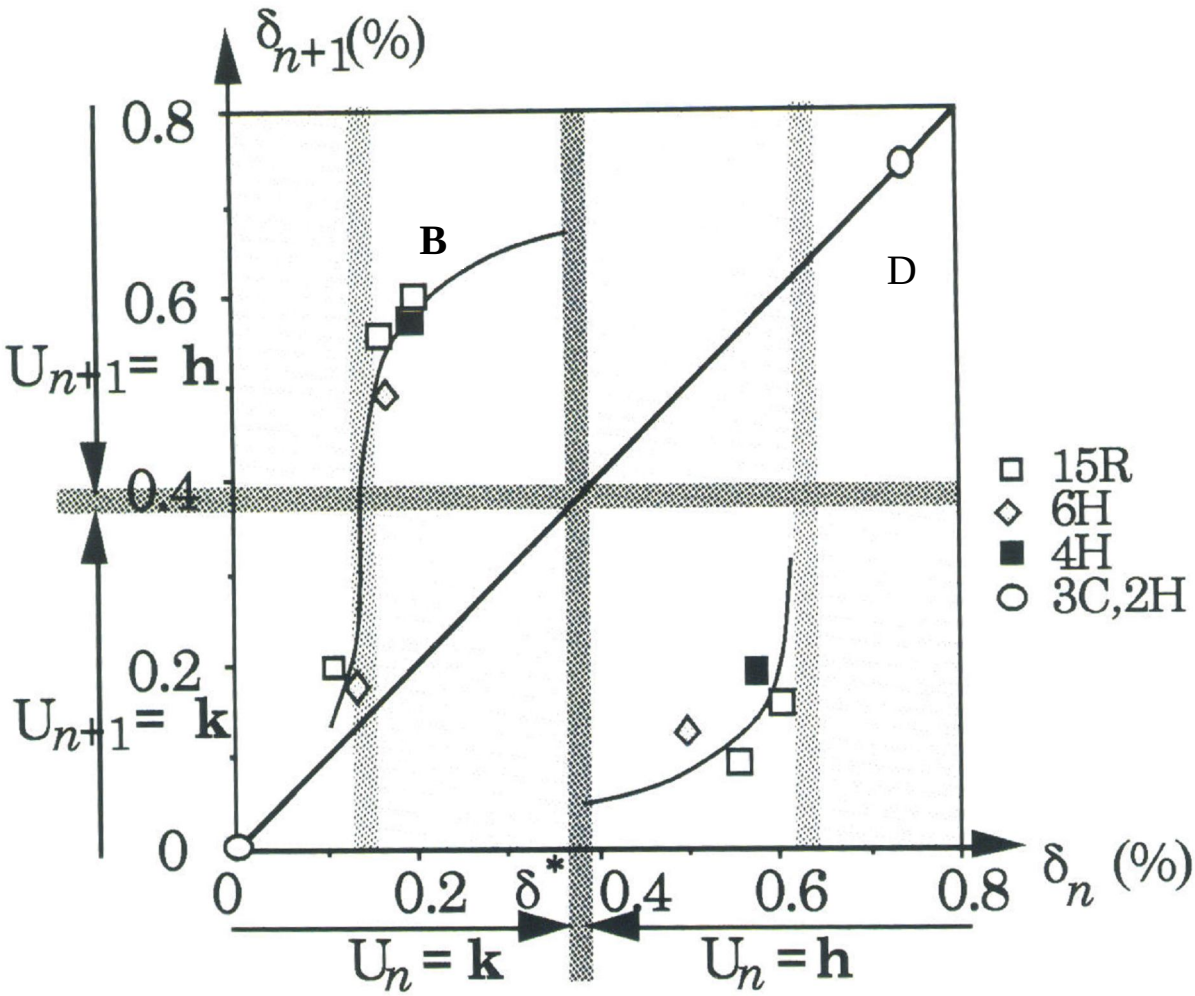
δn+1(%)
0.8
0.6
0.4
0.2
0
Un+1= h
Un+1= k
B
D
15R
6H
4H
3C,2H
0
0.2
δ*
0.4
0.6
0.8
δn (%)
Un = k
Un = h

Figure 4.

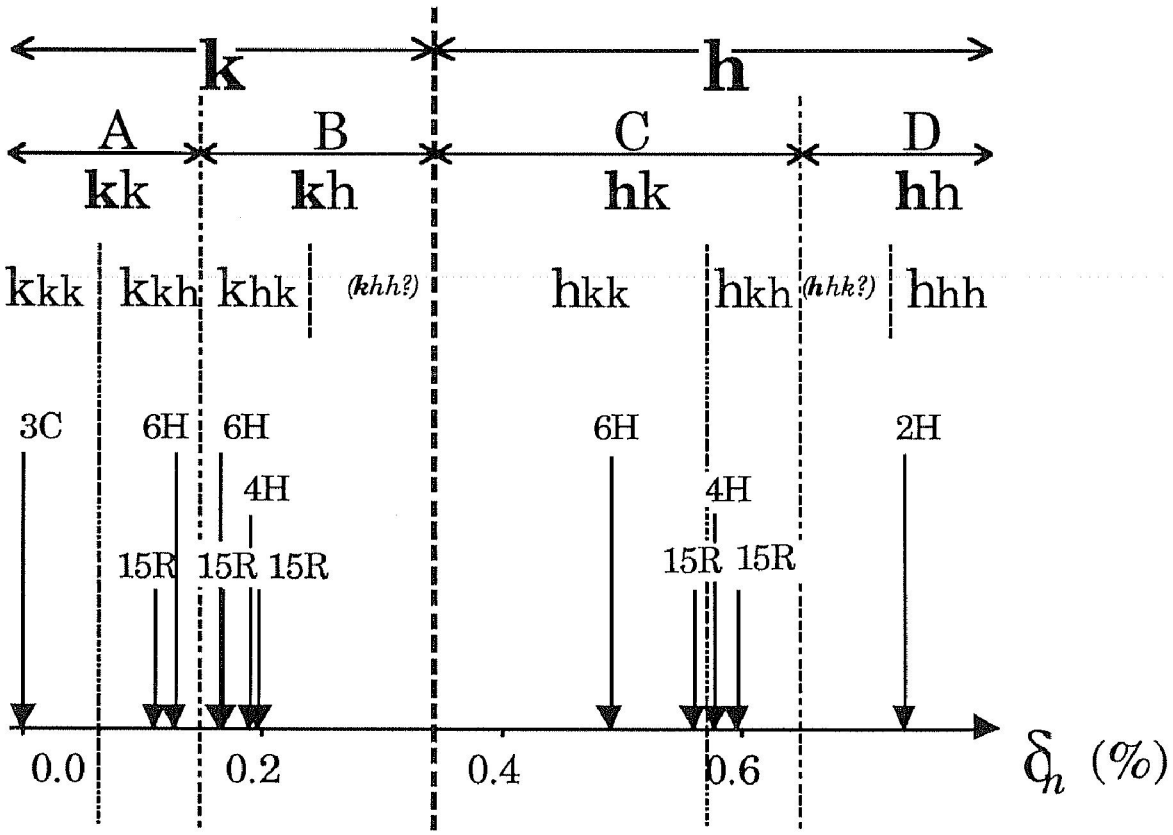
k
h
A
B
C
D
kk
kh
hk
hh
kkk
kkh
khk
(khh?)
hkk
hkh
(hhk?)
hhh
3C
6H
6H
4H
15R
15R
15R
6H
4H
15R
15R
2H
0.0
0.2
0.4
0.6
δn (%)

Figure 5.

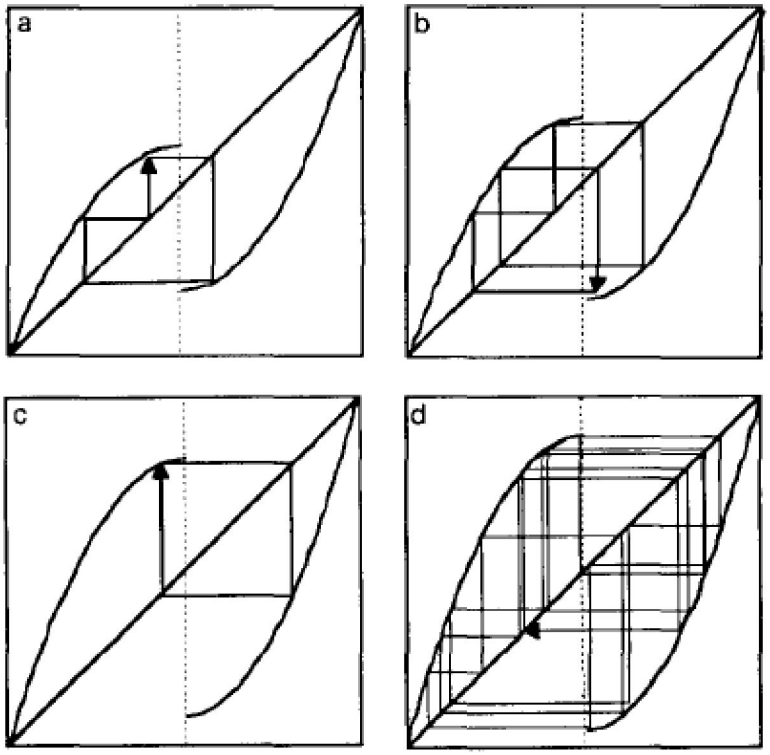

Figure 6.

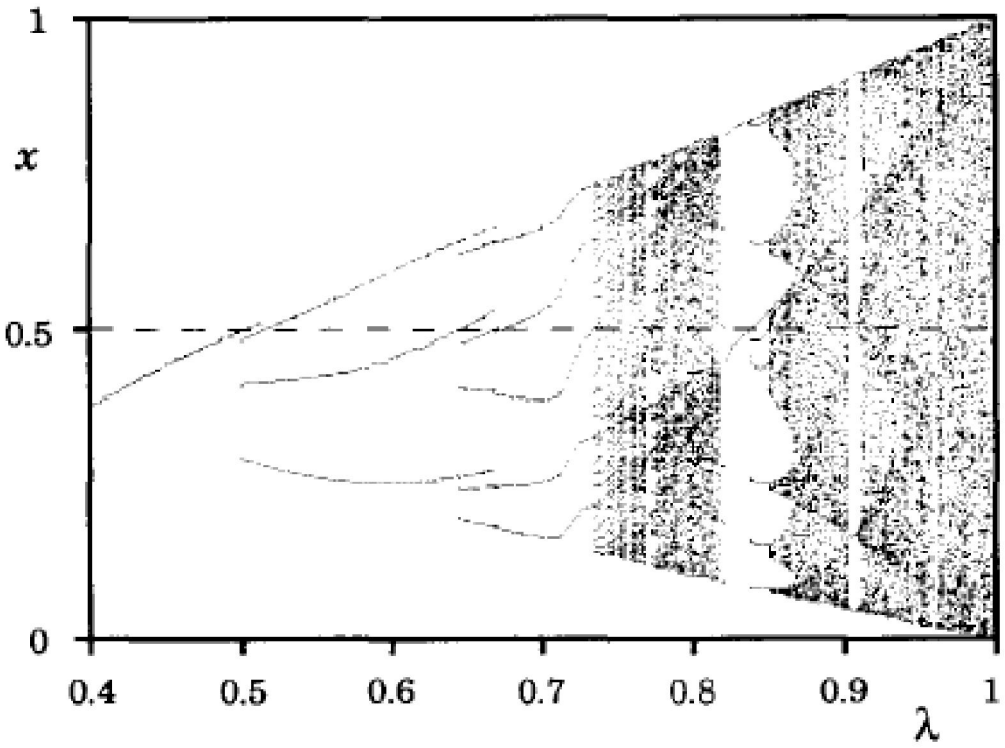

Figure 7.